JOURNAL OF MATERIALS SCIENCE 31 (1996) 2065–2069

Damage and fracture of a cross woven C/SiC composite subject to compression loading

MINGDE WANG, C. LAIRD
Department of Materials Science and Engineering, University of Pennsylvania, Philadelphia, PA 19104-6272, USA

In order to understand the mechanical behaviours of ceramic matrix composites under various loading conditions, the compression stress–strain behaviour of a cross woven C/SiC ceramic matrix composite was characterized in terms of damage and fracture mechanisms, which were observed by scanning electron microscope (SEM) on a side-polished sample. The compression stress–strain curve was found to consist of two stages. The first stage, which extends to about 300 MPa, covers linear elastic deformation with a compression modulus of 140 GPa. The second stage starts with the occurrence of compression damage modes, which include ply delamination, bundle separation and transverse bundle cracking. Depending on the local structure of the sample, the second stage of the stress–strain curve can be either mostly linear or non-linear. The fracture of the composite under compression is by kinking, shearing and bending fracture of fibre bundles individually or in groups, forming a macroscopic shear band in the sample.

1. Introduction

The compression properties of ceramic matrix composites (CMC) are of great importance to designers because the application of these composites as structural materials will involve compression, wear and impact, e.g. as heat shields for space vehicles [1]. For unidirectional or cross-ply composites, compressive damage and fracture often involve longitudinal (or axial) splitting, buckling, kink banding or shear banding [2–4]. These types of damage and fracture modes can occur alone or in combination in CMCs, depending on the laminate lay-up, fibre/matrix interface, and loading conditions. For example, the study by Lankford [3] indicated that longitudinal splitting occurred first in the matrix between the fibres, when a unidirectional ceramic composite was compressed at ambient temperature in regular atmosphere, and was followed by both buckling and kinking of the fibres, leading to composite failure. When the same kind of composite was confined by hydrostatic pressure, the composite failed in shear banding. However, in unidirectional or cross-ply composites, compression damage and fracture often take place instantaneously, making the associated stress–strain curves mostly linear, i.e. the composite fails without warning, much like a brittle material.

Textile ceramic composites, which are more complicated in structure than unidirectional or cross-ply composites, show a quite different compression stress–strain behaviour. Compression loading of cross-woven ceramic composites have indicated a substantial non-linear portion in the stress–strain curve before failure [5]. In another study [6], matrix fragmentation and buckling of fibre bundles were found to be responsible for the gradual fracture of the cross-woven C/SiC composite. However, the effect of the complex microstructures in the textile composites on the compression damage and fracture and, thus, the compression stress–strain behaviour has not been investigated in these two studies.

In the present study, the compression behaviour of a cross-woven C/SiC ceramic composite was studied in terms of damage and fracture occurring in the composite sample. We also treat the effect of existing microstructure variability on compression behaviour of the experimental composite.

2. Materials and experimental procedures

The experimental material used in this study is a cross-woven C/SiC composite supplied by DuPont Co. The composite consists of thirteen plies of unbalanced cross-woven fabric with the fibre count ratio in the longitudinal direction to the transverse direction equal to 6:1. The SiC matrix in the composite was deposited by chemical vapour infiltration (CVI) through a proprietary procedure. The microstructure of the composite is described in detail in a previous paper [7], thus, only those microstructural features relevant to the present study are summarized in the following.

Fig. 1 shows the typical microstructure of the C/SiC composite in the longitudinal direction. From this figure, it is seen that the longitudinal bundles in the composite undulate, and the undulations of the longitudinal bundles are not in synchrony with each other (e.g. the first and second bundles from the top surface

0022–2461

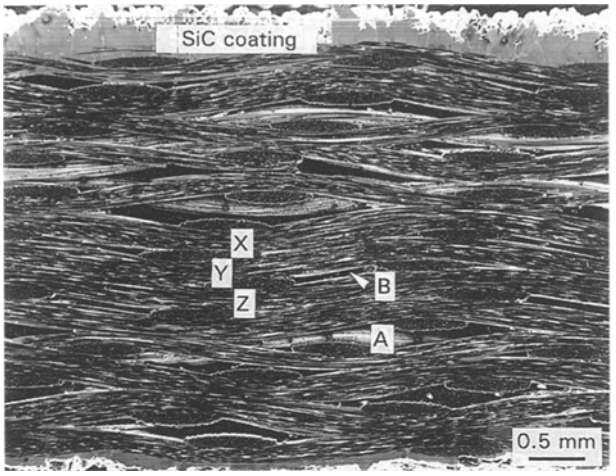

Figure 1 Longitudinal cross-section of C/SiC composite, showing coating layers on both sample surfaces and interbundle voids (A and B). Bundles X and Y were laid up mostly through transverse bundles while Y and Z have extensive longitudinal contacts.

in Fig. 1), indicating that the fabric plies were haphazardly stacked on top of each other in the laying up process. This lay up is termed "random phase lay up". This random phase lay up caused variations in the contacts of the plies, i.e. some plies were laid up through transverse bundles (X and Y in Fig. 1), other plies were laid up through various degrees of longitudinal bundle contacts (Y and Z). Another consequence of this random phase lay up is the non-uniform distribution and size variation of the interfibre voids (e.g. A and B in Fig. 1). Because of the complex microstructures of the composite, the volume fractions of the fibre, matrix and void can only be estimated [7] and are about 53%, 34% and 13%, respectively.

The composite contains thick SiC coatings on both surfaces (Fig. 1) and thin SiC coatings on fibre bundles [7]. Processing related cracks were also found in those coatings and in the transverse fibre bundles. Such cracks were caused by the thermal expansion mismatch between the carbon fibres and SiC matrix during cool down from the CVI processing temperature. These cracks can be quantified as "surface coating crack density", "bundle coating crack density", and "transverse bundle crack density". Measurements of the first two, which were also described in reference [7], give results in numbers of cracks per unit length (no./mm). The transverse crack density was obtained by averaging the number of cracks in 50 transverse bundles, and defining a number as cracks per bundle (i.e. no./bdl). All these crack densities were obtained for the compression test before testing and after successive applications of stress: 150 and 315 MPa on a side polished sample.

The specimen used in the compression test was a composite strip of length of 65 mm, width of 4 mm and thickness of 4.4 mm. Both ends of the specimen were tabbed using clear polyester resin. Compression testing was carried out on an Instron 1361 screw-driven universal testing machine. The test frame was equipped with a MTS hydraulic grip system. The alignment of the grip was well tuned and regularly checked by gripping a flat glass slide and pulling it to failure. Strains were measured using an Instron dynamic extensometer with a gauge length of 10 mm. To avoid extensometer slippage during the test, the extensometer knife edges were glued to the specimen using a 5 min epoxy. The compression load and displacement signals were recorded using a X–Y recorder and a data acquisition system running on an IBM PC.

Monotonic compression tests were conducted in stroke control using linear ramp loading. The stroking rate was 10^{-2} mm s^{-1}. Loading–unloading tests (step tests) with compression stresses of 150 and 315 MPa were also conducted to observe damage modes, to measure crack densities on a side polished sample, and to study the change of composite modulus with compression stress. The same loading conditions as used in the monotonic tests were used for these step tests.

From the compression tests, Young's modulus was obtained by linear fitting of the initial linear part of the stress–strain curve. In the step test, the loading stress–strain curve was found to be linear up to the load level of the preceding step. The composite modulus was obtained by curve fitting the linear portion of the loading curve.

Compression damage modes and fracture modes were examined in the scanning electron microscope (SEM) on samples, with one side polished, which were unloaded from 315 MPa and after the sample failed.

3. Results

The compression stress–strain curve for the C/SiC composite, shown in Fig. 2, occurs in two parts. The first is a linear part which extends to a stress of about 310 MPa. The compression modulus obtained from this part is 140 GPa. The second part is also approximately linear with a very low slope. The sample failed at the compression strength of 345 MPa, and the corresponding failure strain is 0.295%. The final failure of the sample was signalled by a sudden drop of load to very low stress.

The stress–strain behaviour in the compression test of C/SiC composites indicates probable composite damage at the change of slope (Fig. 2). To prove this speculation, a compressive load–unload test was

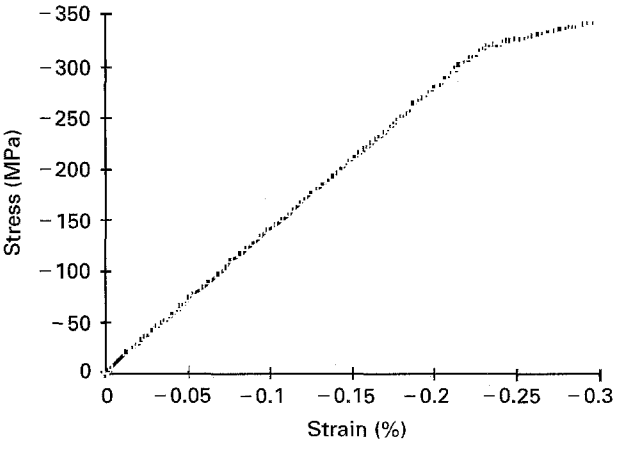

Figure 2 Compression stress–strain curve of C/SiC composite.

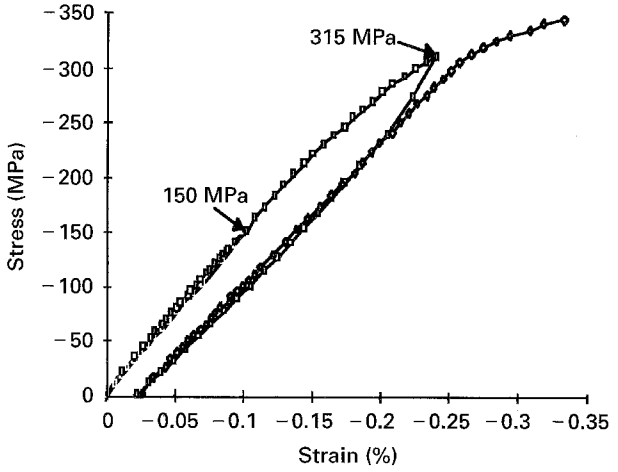

Figure 3 Step-loading compression stress–strain loops for C/SiC composite indicating residual strain after being unloaded from 315 MPa.

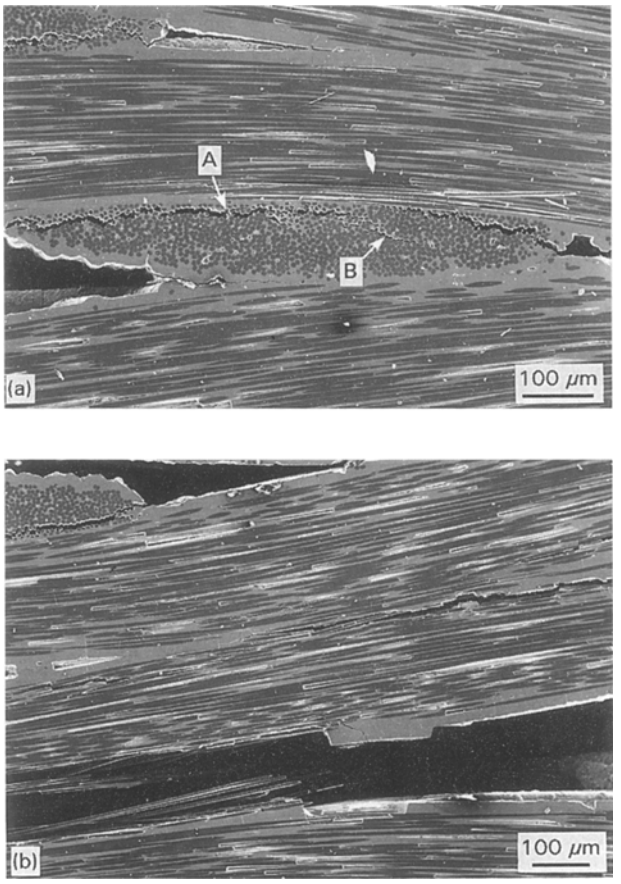

Figure 4 SEM micrographs of a sample compressed at 315 MPa, showing: (a) separation between transverse bundle and longitudinal bundle (A) and shear cracking in transverse bundle (B); (b) ply delamination between two longitudinal bundles.

conducted using stress levels of 150 MPa (at which the stress–strain is still linear), and 315 MPa, right after the decrease of slope. Fig. 3 shows the loading–unloading stress–strain loops, and it is seen that, at 150 MPa, the loading and unloading curves are almost the same, indicating that no damage has been done in the sample. Subsequent reloading is linear up to around 300 MPa, and then, the curve becomes non-linear instead of abruptly changing to a linear portion with a low slope, as in the monotonic compression curve (Fig. 2). Unloading from 315 MPa resulted in a hysteresis loop with a residual strain of 0.024%. The third loading curve is linear up to about 315 MPa (stress level of the previous loading step) after which the slope decreases until failure occurs in the same manner as in monotonic compression.

The variation of the composite modulus is listed in Table I as a function of the compression stress. Table I also contains crack densities measured on the surface coating, the longitudinal bundle coating and in transverse bundles at 0, 150 and 315 MPa. It is seen from Table I that, at 150 MPa, the modulus and all the crack densities showed no change from the as-received state, confirming that no damage was done to the composite. At 315 MPa, on the other hand, the modulus decreased and the transverse bundle crack density increased while the other two crack densities showed very limited increase. The compression strength and failure strain for the step loading sample were measured as 348 MPa and 0.331%, respectively.

Compression damage modes were identified using SEM on a polished sample unloaded from 315 MPa. Those damage modes are: (i) separation between transverse bundles and longitudinal bundles of the same fabric ply (A in Fig. 4a), (ii) shear cracking of transverse bundles (B in Fig. 4a and Table I), and (iii) delamination between fabric plies (Fig. 4b). Matrix cracking in terms of crack multiplication in the composite surface coating and longitudinal bundles was very limited, as indicated in Table I. Moreover, most of the processing-related cracks existing in the longitudinal bundles and sample surface coating were found to have not propagated at the compression stress of 315 MPa [8]. Therefore, the three damage modes observed are mostly responsible for

TABLE I Composite modulus and averaged crack densities after loading to different compression stresses

Stress (MPa)	Modulus (GPa)	Surface[a] (mm^{-1})	Longitudinal bundle[b] (mm^{-1})	Transverse bundle[c] (mm^{-1})
0	144	2.61	2.93	0.65
150	143	2.62	2.93	0.65
315	132.8	2.79	3.11	1.07

[a] Surface coating crack density.
[b] Bundle coating crack density.
[c] Transverse bundle crack density.

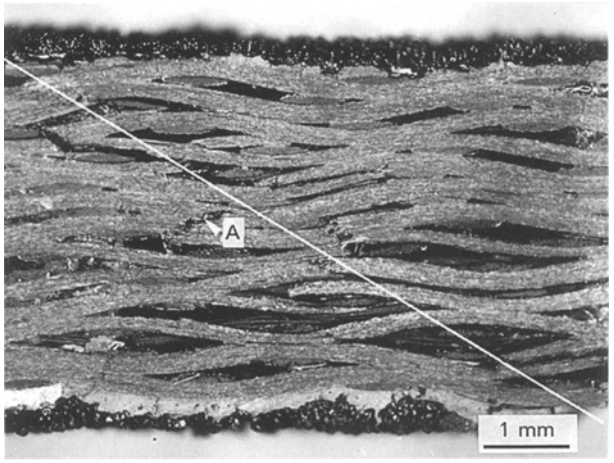

Figure 5 Optical micrograph showing compression fracture of a C/SiC composite. Note that longitudinal bundles fracture in groups of two (A) and they lie about a macroscopic shear plane across the sample, indicated by the oblique line.

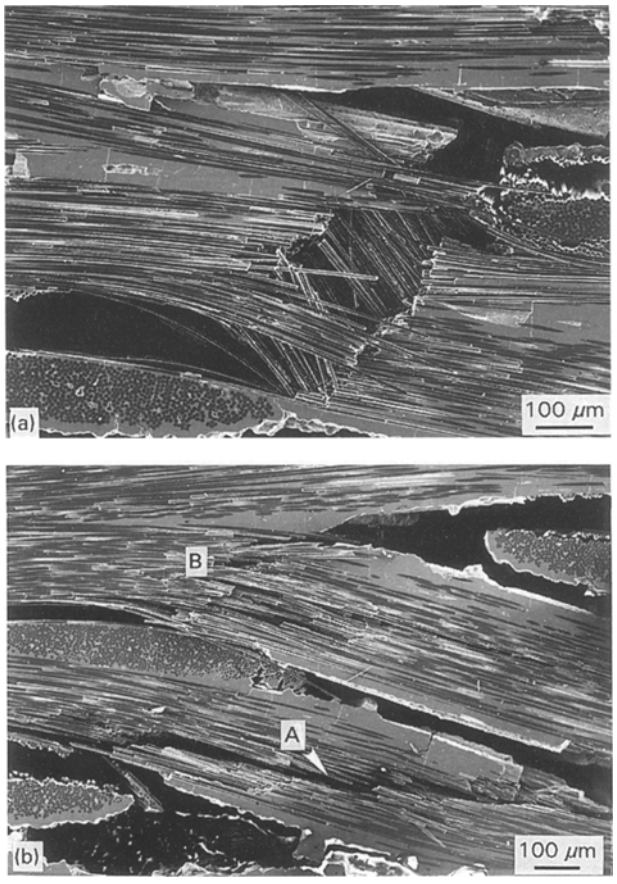

Figure 6 SEM micrographs showing: (a) kink banding of a longitudinal bundle; (b) shear fracture (A) and bend fracture (B) of a longitudinal bundle.

the reduction of the compression modulus as indicated in Table I.

The failure of the composite under compression is by fracture of longitudinal bundles, as shown in Fig. 5. As seen from Fig. 5, most of the fracture of the longitudinal bundles takes place in groups of two neighbouring bundles (e.g. A Fig. 5). It is also noted that the bundle fracture often occurs in places where there are large interbundle voids nearby, as indicated by A in Fig. 5. Although the bundle fracture groups seem to be independent of each other, they actually lie about a macroscopic shear fracture plane of the composite (Fig. 5). Examination of the fracture modes of the longitudinal bundles at higher magnifications revealed that there are three types. The first, shown in Fig. 6a, is bundle kinking. The second is bundle shear fracture and the third, bending fracture, which are shown in Fig. 6b as A and B, respectively. From the manner of the bundle fracture, it is unlikely that these failed bundles can bear any load. Therefore, when a bundle fails, the bundles that used to be physically connected with it will fail at overload, forming a fracture group. The compression fracture initiates and propagates suddenly and locally.

4. Discussion

The overall compression stress–strain behaviour of the cross-woven C/SiC composite can be related to the deformation, damage and fracture occurring locally in the composite, as schematically shown in Fig. 7. In the elastic region (Fig. 7a), the composite shortens and the individual bundles attempt to buckle due to the undulations induced by bundle weave and the existence of the large interbundle voids. Compared to tension behaviour [7], the elastic region in compression extends to much higher stress levels (about 300 MPa in compression versus about 50 MPa in tension). This is because, in tension, the processing related cracks started to propagate at low stress levels of 50 MPa [7], while in compression, the propagation of these cracks was very limited even at 315 MPa [8]. However, the moduli obtained from the initial elastic stage of both tests are nearly the same, i.e. about 140 GPa. This indicates that the measured modulus is a characteristic value of the experimental cross-woven C/SiC composite. This also indicates that the processing related cracks on both the composite surface coating and the longitudinal bundles did not close up during compression to give a high modulus. This is

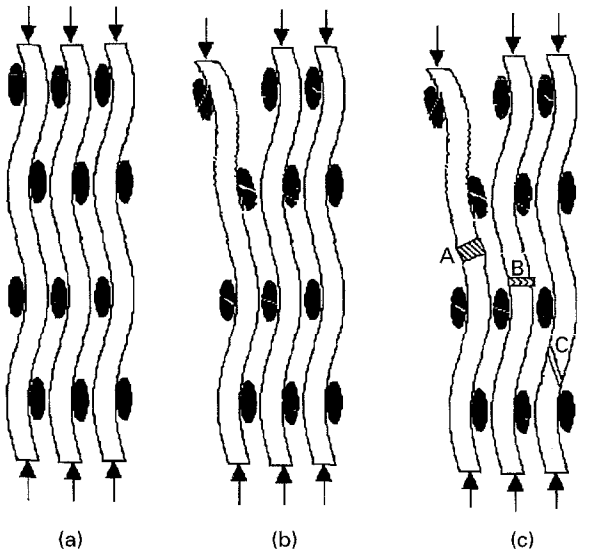

Figure 7 Schematic of compression deformation and fracture. (a) elastic shortening; (b) compression damage in terms of ply delamination, bundle separation in the same layer, and transverse bundle shear cracking, due to bundle buckling; (c) failure of the composite by kinking (A), bend fracture (B), and shear fracture (C) of longitudinal bundles.

probably because of the fact that the bundles deform by buckling due to the undulations (Fig. 7a), which prevents the processing-related cracks from closing up, and the fact that these cracks may touch at a few spots, so that they do not have to close under compression. Therefore, it is apparent that step loading to 150 MPa did not change the modulus and the damage status, as shown in Table I.

When the compression stress reaches above 300 MPa, damage takes place in terms of separation of transverse bundles from longitudinal bundles in the same ply, ply delamination and transverse bundle shear cracking (Fig. 4a and b). This is because the buckling of bundles at this stress level can generate high enough tensile stresses between bundles and plies to cause the damage (schematically shown in Fig. 7b). This damage process could be sudden and massive, as in the monotonic test, or could be more gradual as in the step test. After the damage, the longitudinal bundles can deform more readily by buckling because the damage relieves the constraint acting on them, leading to a low slope in the stress–strain curve (Figs 2 and 3) and a decrease of composite modulus (Table I). At the same time, the stress states in the composite are changed due to this damage such that limited matrix cracking in the composite can take place (Table I), contributing to modulus reduction. When the applied stress reaches about 345 MPa, the composite fails by the kinking, shearing, and bending fracture of the longitudinal bundles (Fig. 6a and b, and schematically in Fig. 7c). While kinking and shearing are typical compression fracture modes observed in many composite systems [2–4], the bending fracture is produced as the combined effect of local bundle undulation, microstructural inhomogeneities, and chance contacts with surrounding microstructural features. As in other composite systems, the above-described compression fracture modes initiate and propagate instantaneously, leading to a sudden failure of the composite.

In monotonic compression, the damage developed at a stress a little above 300 MPa in a sudden and massive manner, resulting in a sharp decrease of slope in the stress–strain curve (Fig. 2). Whereas in the step loading test, the damage occurred more gradually, starting at a little below 300 MPa, causing a nonlinear stress–strain curve (Fig. 3) and producing a higher failure strain (accumulative) than in the monotonic test (0.331% for the step test versus 0.295% for the monotonic test). We believe that these differences are representative of scatter expected in the mechanical tests and can be explained as follows. Of the three damage modes which determine the second part of the stress–strain curve, ply delamination can be directly related to the contacts of bundles between the fabric plies. Due to the random phase lay up existing in the present composite (Fig. 1), the "density" (i.e. number per volume) and the nature (between longitudinal bundles or between transverse and longitudinal bundles) of those contacts are expected to be different from sample to sample. Moreover, the undulations of the bundles might also be different from bundle to bundle and from sample to sample. Therefore, the differences in the local lay-up of plies and bundle undulations in these two samples result in different compression stress–strain behaviour. It is also reasonable to suggest that the composite local structure is responsible for the stress level and the detailed mechanism by which the damage could develop in compression.

5. Conclusions

1. The compression behaviour of the cross-woven C/SiC composite consists of two distinctive stages. In the first stage, the composite shortens elastically without damage up to a stress of about 300 MPa. In the second stage, compression damage occurs in the composite as ply delamination, separation of transverse bundles and longitudinal bundles in the same ply, and shear cracking in the transverse bundle. These types of damage cause the slope of the stress–strain curve to decrease dramatically. The failure of the composite under compression is due to the kinking, shearing and bending fracture of longitudinal bundles. These bundle fractures often involve two bundles as a group and lie in the macroscopic shear plane of the composite.

2. The occurrence and accumulation of the compression damage modes are sensitive to the local structures in the gauge section in terms of contacts with neighbouring bundles and interbundle voids. Such local structural features vary from bundle to bundle, due to the random phase lay up of the cross-woven fabric ply. As a consequence of the microstructural variations, minor differences can be expected in the compression stress–strain curves of individual samples, giving rise to scatter.

Acknowledgement

This work was financially supported by the Benjamin Franklin Program of the Commonwealth of Pennsylvania and the Materials Science Corporation. The authors are deeply grateful for this support. The authors also thank Dr Alex Radin for his expert help in mechanical testing of the composite samples, and Ms Xuqing Wang for her help in SEM. The Laboratory for Research on the Structure of Matter in the University of Pennsylvania is warmly acknowledged for providing the facilities for this work.

References

1. S. R. RICCITIELLO, W. L. LOVE and W. C. PITTS, *SAMPE* (July, 1993) 10.
2. J. LANKFORD, personal communication (1993).
3. *Idem, Comp. Sci. Tech.*, Personal communication.
4. J.-B. HA and J. A. NAIRN, *SAMPE Q.* (April, 1992) 29.
5. J. Y. ROSSIGNOL, J. M. QUENISSET, H. HANNACHE, C. MALLET, R. NASLAIN and F. CHRISTIN, *J. Mater. Sci.* **22** (1987) 3240.
6. Z. WANG, C. LAIRD, Z. HASHIN, B. W. ROSEN and C.-F. YEN, *ibid.* **26** (1991) 4751.
7. M. WANG and C. LAIRD, *Acta Metall. Mater.*, in press.
8. M. WANG, PhD thesis, University of Pennsylvania, Philadelphia, USA (1994).

Received 4 April
and accepted 19 September 1995